Foot pressure distribution in White Rhinoceroses (*Ceratotherium simum*) during walking

Olga Panagiotopoulou [Corresp., 1] , Todd C Pataky [2] , John R Hutchinson [Corresp. 3]

[1] Monash Biomedicine Discovery Institute, Department of Anatomy and Developmental Biology, Moving Morphology & Functional Mechanics Laboratory, Monash University, Clayton, Victoria, Australia

[2] Department of Human Health Sciences, Kyoto University, Kyoto, Japan

[3] Department of Comparative Biomedical Sciences, Structure and Motion Laboratory, Royal Veterinary College, Hatfield, United Kingdom

Corresponding Authors: Olga Panagiotopoulou, John R Hutchinson
Email address: olga.panagiotopoulou@monash.edu, JHutchinson@rvc.ac.uk

White rhinoceroses (*Ceratotherium simum*) are odd-toed ungulates that belong to the group Perissodactyla and are second only to elephants in terms of large body mass amongst extant tetrapods, making them fascinating studies for how large land animals support and move themselves. Rhinoceroses often are kept in captivity for protection from ivory poachers and for educational/touristic purposes, yet a detrimental side effect of captivity can be foot disease (i.e. enthesopathies and osteoarthritis around the phalanges). Foot diseases in large mammals are multifactorial, but locomotor biomechanics (e.g. pressures routinely experienced by the feet) surely can be a contributing factor. However, due to a lack of *in vivo* experimental data on rhinoceros foot pressures, our knowledge of locomotor performance and its links to foot disease is limited. The overall aim of this study was to characterize peak pressures and centre of pressure trajectories in white rhinoceroses during walking. We asked two major questions. First, are peak locomotor pressures the lowest around the fat pad and its lobes (as in the case of elephants)? Second, are peak locomotor pressures concentrated around the areas with the highest reported incidence of pathologies? Our results show a reduction of pressures around the fat pad and its lobes, which is potentially due to the material properties of the fat pad or the fact that our rhinoceros subjects avoided "heel" contact at impact. We also found an even and gradual concentration of foot pressures across all digits, which may be a by-product of the more horizontal foot roll-off during the stance phase. While our exploratory, descriptive sample precluded hypothesis testing, our study provides important new data on rhinoceros locomotion for future studies to build on, and thus impetus for improved implementation in the care of captive/managed rhinoceroses.

1

2   **Title**: Foot pressure distribution in White Rhinoceroses (*Ceratotherium simum*) during walking.

3   **Authors**: Olga Panagiotopoulou[1], Todd C Pataky[2], John R Hutchinson[3]

4   1. Monash Biomedicine Discovery Institute, Department of Anatomy and Developmental Biology,
5   Moving Morphology & Functional Mechanics Laboratory, Monash University, Victoria,
6   Australia
7   2. Department of Human Health Sciences, Kyoto University, Kyoto, Japan
8   3. Department of Comparative Biomedical Sciences, Structure and Motion Laboratory,
9   The Royal Veterinary College, Hatfield, UK
10
11
12
13   Corresponding authors:
14   Dr Olga Panagiotopoulou (olga.panagiotopoulou@monash.edu)
15   Professor John R Hutchinson (JHutchinson@rvc.ac.uk)
16
17

18   **Abstract**

19   White rhinoceroses (*Ceratotherium simum*) are odd-toed ungulates that belong to the group
20   Perissodactyla and are second only to elephants in terms of large body mass amongst extant tetrapods,
21   making them fascinating studies for how large land animals support and move themselves. Rhinoceroses
22   often are kept in captivity for protection from ivory poachers and for educational/touristic purposes, yet
23   a detrimental side effect of captivity can be foot disease (i.e. enthesopathies and osteoarthritis around the
24   phalanges). Foot diseases in large mammals are multifactorial, but locomotor biomechanics (e.g.
25   pressures routinely experienced by the feet) surely can be a contributing factor. However, due to a lack
26   of *in vivo* experimental data on rhinoceros foot pressures, our knowledge of locomotor performance and
27   its links to foot disease is limited. The overall aim of this study was to characterize peak pressures and
28   centre of pressure trajectories in white rhinoceroses during walking. We asked two major questions.
29   First, are peak locomotor pressures the lowest around the fat pad and its lobes (as in the case of
30   elephants)? Second, are peak locomotor pressures concentrated around the areas with the highest
31   reported incidence of pathologies? Our results show a reduction of pressures around the fat pad and its
32   lobes, which is potentially due to the material properties of the fat pad or the fact that our rhinoceros
33   subjects avoided "heel" contact at impact. We also found an even and gradual concentration of foot
34   pressures across all digits, which may be a by-product of the more horizontal foot roll-off during the
35   stance phase. While our exploratory, descriptive sample precluded hypothesis testing, our study provides
36   important new data on rhinoceros locomotion for future studies to build on, and thus impetus for
37   improved implementation in the care of captive/managed rhinoceroses.

38
39   **Keywords:** biomechanics, Perissodactyla, locomotion, osteopathology, mechanobiology, gait

40
41   **Introduction**

42   Over millions of years of evolution, the feet of rhinoceroses have had to change with other alterations of
43   limb morphology, locomotor behaviour, body size, habitat and more (e.g. Prothero, 2005; Stilson et al.,
44   2016). Extant rhinoceroses include the second largest (after elephants) extant terrestrial mammals, with
45   body masses in the White rhinoceros reaching up to 3600 kg (Groves 1972; Hiilman-Smith et al., 1986;
46   Owen-Smith 1992), so in large rhinoceroses locomotor stresses might be considerable if not well-controlled,
47   imposing severe biomechanical constraints on form and function (Alexander and Pond, 1992). Contrary to
48   feet of elephants, which bear five functional digits and "predigits" (Hutchinson et al., 2011; Mariappa, 1986;
49   Neuville, 1935; Weissengruber et al., 2006), rhinoceros feet have three digits (numbered II-IV) terminating
50   in horns/hooves (Prothero, 2005; Regnault et al., 2013) and no supportive "predigits". Of the three digits,
51   digit II and IV respectively dominate the medial and lateral aspects of the foot, whilst digit III is the central
52   and largest of all. Each digit consists of three phalanges (proximal, medial and distal) and the foot caudally
53   and centrally is enclosed in a fat pat. The bilobed fat pad is structurally similar but smaller in size to elephant
54   fat pads and expands when compressed (von Houwald 2001). This structure potentially helps to evenly
55   distribute locomotor stresses across the sole of the foot, as in the case of elephants (Panagiotopoulou et al.,
56   2012, 2016). Overall, the morphology of rhinoceros feet is fairly symmetrical from medial to lateral; unlike
57   the feet of elephants which are more robust laterally (e.g. digits III-V).

58
59   Considering that large mammals' feet support their body mass during gait, understanding healthy foot
60   function is important for understanding healthy gait. This is particularly important in view of documented
61   rhinoceros foot pathologies (Dudley et al., 2014; Flach et al., 2003; Galateanu et al., 2013; Harrison et al.,
62   2011; Jacobsen, 2002; Jones 1979; Regnault et al., 2013; Von Houwold 2001; Von Houwald and
63   Guldenschuh 2002; Von Houwold and Flach, 1998; Zainuddin et al., 1990). Previous research on museum
64   specimens found a high occurrence of enthesopathies and osteoarthritis on the phalanges of rhinoceros feet
65   (Regnault et al., 2013)-- of the 81 feet from 27 rhinoceroses studied, 54 feet from 22 individuals exhibited
66   osteopathologies (Dudley et al., 2014). Surprisingly, limb osteopathologies have remained remarkably
67   common in rhinocerotid species across their evolution but increasing with estimated body mass, consistent

68 with tradeoffs and compromises between large size, cursorial/medioportal morphology or athletic capacity,
69 and limb health (Stilson et al., 2016).
70
71 Many factors can cause foot disease in large mammals, but previous research in elephants has linked foot
72 disease with obesity, space limitations and the time the animals spent walking or standing on hard
73 (unnatural) surfaces (Csuti et al., 2001; Fowler and Mikota 2006; Miller et al., 2016). Our prior studies
74 proposed that elephants normally have high pressures laterally, on digits III-V (Panagiotopoulou et al., 2012,
75 2016), congruent with where elephants tend to exhibit greater incidences of osteopathologies (Regnault et
76 al., 2017). In contrast, there are almost no *in vivo* studies of locomotion in rhinoceroses (e.g. Alexander and
77 Pond, 1992), in any aspects including the pressures experienced by the feet. Based on the roughly equivalent
78 occurrence of osteopathologies across rhinoceros digits II-IV (Regnault et al., 2017), we expect that
79 pressures would be evenly distributed across these digits too, and for pressures to be low on the fat pad
80 lobes; without the mediolateral asymmetry of pathologies or pressures observed in elephant feet.
81
82 In this pilot study, we describe *in vivo* locomotor foot pressures and centre of pressure trajectories (COP) in
83 three white rhinoceroses (*Ceratotherium simum*) during walking. Our limited sample size does not allow us
84 to conduct hypothesis testing on foot pressure magnitudes. However, we were able to conduct preliminary,
85 qualitative evaluation of our two hypotheses, for future studies to expand on:
86
87 Hypothesis I. Peak locomotor pressures will be the lowest in the central and caudal parts of the foot at the
88 locations of the fat pad and its lobes. This is expected from a dynamic interaction of behavioural walking
89 preferences (manifested in COP) and the compliant properties of the fat pad, as we have previously observed
90 in elephants (Panagiotopoulou et al., 2012, 2016).
91
92 Hypothesis II. Peak locomotor pressures will be concentrated equally around the horns/hooves and
93 phalangeal pads of all digits (II-IV), which correspond to the overlying bony areas with the highest evidence
94 of osteoarthritis and similar pathologies (Regnault et al, 2013); without a strong tendency for more lateral
95 prevalence of pathology.
96
97
98 **Methods**
99 Subjects
100 Two adults and a juvenile captive southern White Rhinoceros (*Ceratotherium simum*) from Colchester Zoo
101 (Colchester, UK) participated in the study (Table 1). The body masses of the subjects were estimated by the
102 zoo keepers using the zoo's records. Zoo keepers and veterinarians gave clinical consent for the study and
103 all animal participants were healthy. The study was approved by The Royal Veterinary College's Animal
104 Ethics Committee (approval number URN 2010 1052).
105
106 Data collection
107 A 5m walkway was constructed in a crush area in the rhinoceros enclosure (Figure 1A). A 3m long and
108 0.4m wide foam pad was laid at the beginning of the walkway and was followed by a 1.0 x 0.4m pressure
109 plate (fitted with 8192 sensors, 2.05 sensors cm^{-2}) (Footscan; RSscan, Olen, Belgium), and a 1m length of
110 foam pad. The walkway was covered with a 0.3mm thick rubber mat to prevent the animals from
111 recognising the location of the pressure plate. Reflective tape was placed on the rhinoceros hip and shoulder
112 to calculate walking speeds using a Sony HDR (Sony, London, UK) high definition video camera. The
113 camera was placed perpendicular to and at a 2m distance from the walkway. Camera and pressure plate
114 sampling frequencies were respectively 25Hz and 250Hz. The pressure plate was calibrated using a known
115 weight (~95kg human standing on the plate) as per manufacturer's instructions. While we do report absolute
116 pressure magnitudes, the main outcome of interest was the relative (i.e. within-foot) pressure distribution,
117 as this reflects foot functionality. Absolute pressure errors are unexpected to affect relative pressure values.
118 The rhinoceros were guided over the walkway using food as encouragement, an average of 20 times each.

119   Trials with obvious acceleration and deceleration (as judged by video) during data collection were excluded
120   from further analysis (Panagiotopoulou et al., 2012, 2016). Animal discomfort was kept to the minimum
121   by stopping data collection when animals appeared disengaged.
122
123   Data processing
124   Data analysis protocols were similar to Panagiotopoulou et al., (2012, 2016), implanted in Canopy v. 2.1.8
125   using SciPy v. 0.19, NumPy 1.11.3 and Matplotlib 2.0 (Enthought Inc., Austin, TX, USA). In brief, the raw
126   pressure data (x,y,time) of the individual footsteps were exported from the Footscan system, isolated
127   algorithmically using spatio-temporal gaps between clusters of non-zero pressure voxels and were assessed
128   for spatial and temporal completeness as per Panagiotopoulou et al., (2012, 2016). Individual images
129   representative of spatio-temporally complete footsteps were manually identified as fore/hind, right/left;
130   spatially scaled by a factor of 1.5, using bilinear interpolation to compensate for the non-square
131   measurement grid of the RSscan system (7.62 x 5.08 mm, manufacturer specified) and spatially registered
132   within subjects and feet (see Panagiotopoulou et al., (2012)). Following scaling and registration, nine
133   anatomically homologous regions of interest (ROIs) were selected on the mean images for each foot as per
134   Panagiotopoulou et al., (2012, 2016), and peak pressures (N cm^{-2}) of the whole stance phase were extracted
135   from a three-pixel radius using a Gaussian kernel mean window with a standard deviation of one pixel.
136   ROIs 1-3 respectively represented the horns of digits II-IV, ROIs 4-6 represented the (inter)phalangeal pads
137   of digits II-IV respectively, ROI 7 represented the caudal most ("heel") aspect of the sole and ROIs 8-9
138   were respectively placed on the medial and lateral footpads of the sole (Figure 1B). Centre of pressure
139   trajectories (COP) were computed as the pressure-weighted image centroids' time series after thresholding
140   the images at 5 kPa. Due to the limited number of subjects and steps, the dependent variables were not
141   tested for significance. This was a preliminary, qualitative study of rhinoceros foot function during gait, so
142   we neither derived nor tested a null hypothesis.
143

144   **Results**

145   The mean walking speed of all three subjects was 0.53ms^{-1} (Table 1), which corresponded to a mean Froude
146   number (Alexander & Jayes 1983; Fr = velocity^2 * [9.81 ms^{-2} * shoulder height]$^{-1}$) of 0.013, consistent
147   with a slow walk. The peak pressure data per ROI, subject and feet are shown in Table 1. All peak pressure
148   data are in Supplementary Data 1. The mean peak pressure values for the adult subjects 1 and 3 and all feet
149   were respectively 220 kPa and 180 kPa, whilst the mean peak pressure values of the juvenile subject 2 were
150   9 kPa. The mean peak pressure values for both adult subjects and all feet (200kPa) were respectively 4.7
151   and 2.8 times lower than those previously recorded on African (946 kPa) and Asian elephants (567 kPa)
152   during walking (Panagiotopoulou et al., 2012, 2016). The Asian elephant data were collected using the
153   same RSscan system as in this study, yet the African elephant pressure data were collected using a lower
154   resolution system (Zebris Medical GmbH, Biomechanix, Munich) with 100 Hz sampling frequency, 14,080
155   sensors in total and approximately 0.55 sensors cm^{-2}. Our data showed that, similar to elephants and other
156   quadrupeds, the forefeet had higher mean pressure magnitudes than the hindfeet for all subjects (Table 1).
157
158   Contrary to elephants (Panagiotopoulou et al., 2012, 2016), the rhinoceroses' foot pressures did not follow
159   a consistent pattern between feet. The forefeet for adult subject 2 and the juvenile rhino (subject 2) showed
160   higher pressures around the horn of digits II (ROI 1), III (ROI 2) and IV (ROI 3). Intermediate pressures
161   were recorded around the phalangeal pads of digits II-IV and the lowest pressures around the fad pad (ROIs
162   7-9) (Figures 2 & 3). The highest median foot pressures for the right forefeet of all three rhinoceroses were
163   at the horn of digits III and IV, corresponding to ROIs 2 and 3 (Figures 2 & 4). The lowest median peak
164   pressures were recorded around the fat pad; nevertheless, median peak pressures around the phalangeal
165   pads of all digits were very low. Median pressures for the left hindfeet were the highest for the horn of digit
166   II, followed by ROIs 2 & 3 (Figures 2 & 4). Intermediate median pressures were recorded at ROIs 4, 5 &
167   7 and the lowest peak pressures were computed at ROI 8. Regardless, median peak pressure differences

168 between ROIs 2-9 were minimal (Figure 2 & Supplementary Data 1.) Median peak pressures for the
169 hindfeet of the two adult subjects (subject 1 & 3) gave the highest median peak pressures at the horn of
170 digit II (ROI 1) and intermediate pressures at ROIs 2-4 (Figures 2 & 6). The lowest peak pressures were
171 found at ROIs 5-9.

172 The COP trajectories for all time frames, animal participants and feet are shown in supplementary Figures
173 S1- S8. Most COP traces began at the medial aspect of the foot caudally to the interphalangeal pad of
174 digit II or at the medial footpad of the sole, then shifted caudally around the heel aspect of the sole and
175 finally passed cranially through digit III by toe-off. Contrary to this caudo-medial and centrally-focused
176 pressure pattern, pressure traces in two trials for the hind leftfoot started laterally on digit IV before
177 shifting caudo-cranially and through digit III by toe-off. Thus there was some unusual variability in our
178 subjects' COP traces during normal locomotion.

Discussion

180 Overall, we found reduction of peak pressures around the fat pad, qualitatively supporting our hypothesis I
181 that, like in elephants, rhinoceros fat pads may keep locomotor pressures low due to their compliance.
182 Whilst our quantitative results showed variation in peak foot pressures across feet, we recorded the highest
183 peak pressures around the horn and phalangeal pads of all digits, yet this signal was not as strong for the
184 left hindfoot (Figure 2). Such variations may be due to the ROI method used for data analysis. Although
185 the ROI approach is a widely used technique for the estimation of peak pressure magnitudes sampled from
186 specific anatomical regions, it overlooks variability within regions, assuming that all regions are
187 functionally independent. We have previously shown a significant interaction between the topology of the
188 ROIs and pressure magnitudes in elephants (Panagiotopoulou et al., 2016). Variation in peak pressures
189 between ROIs may also have a biological importance considering that the left hindfoot sometimes showed
190 a lateral-caudal-central roll off pattern, but we remain conservative with any biological conclusions due to
191 our experimental and sample size limitations.

192 The general COP trajectories in our rhinoceros subjects were similar to elephants in being linear during the
193 final half of stance phase rather than sigmoidal as in humans (Lord et al., 1986) and bonobos (Vereecke et
194 al., 2003). However, contrary to elephants, our rhinoceros subjects loaded the medial part of the foot at
195 impact and then shifted their load centrally during mid-stance prior to toe-off via their central digit. Reasons
196 for this apparent preference to avoid "heelstrike", and the strongly medially-biased COP pattern in our
197 subjects early in stance phase, remain unclear; but the variability of COP patterns is cause for caution in
198 attributing this pattern to all rhinoceroses until more such data can be obtained and compared. Hints at other
199 unusual COP patterns – or perhaps subject variability or measurement error – in large mammals (e.g.
200 hippopotamus and tapir COP traces in Figure 1 of Michilsens et al., 2009) are further cause for caution and
201 future analyses.

202 Due to this variation in rhinoceroses' foot pressures and COP trajectories, locomotor patterns are important
203 for assessing peak pressure distributions qualitatively. The peak pressure "heat maps" for all subjects and
204 steps shown in Figures 3-6 indicated a clear concentration of peak pressures around the horn and phalangeal
205 pads of all three digits. These results tentatively support our hypothesis II-- that peak pressures are evenly
206 distributed, rather than biased toward the central and lateral digits, which corresponds to the relatively even
207 distribution of osteopathologies across digits II-IV (Regnault et al., 2013). An even distribution of peak
208 pressures across all three digits might be a by-product of the horizontal position of the foot at impact as
209 manifested by the COP traces (i.e. avoidance of heelstrike). Regardless, large animals such as elephants
210 and rhinoceroses clearly use enlarged foot contact areas to protect the digits from peak pressures that
211 otherwise could cause tissue damage (Chi and Roth, 2010; Michilsens et al., 2009).

212 It is also interesting that forefoot pressures were normally higher in our three subjects, and forefoot
213 osteopathologies tend to be more common than hindfoot osteopathologies (Regnault et al., 2013)—although
214 one study found more chronic foot disease overall in the hindfeet, rather than forefeet, of a sample of One-
215 horned rhinoceroses (von Houwald and Flach, 1998). The latter study posited some biomechanical factors
216 that may underlie foot pathologies, including toe horn-cracking, shearing forces on the middle toe, low
217 friction causing low wear and overgrowth of the middle toe horn, which could inspire future studies building
218 on this one. Regardless, these patterns are opposite those tentatively identified for elephants sampled by
219 Regnault et al. (2017) — they found no clear forefoot vs. hindfoot differences in osteopathologies despite
220 some evidence for higher pressures on elephant forefeet (Panagiotopoulou et al., 2012, 2016). It is tempting
221 to speculate that the more similar morphology and presumably function of all four rhinoceros feet compared
222 with the disparate morphology of elephant fore- vs. hindfeet may explain these discrepancies, but such
223 speculations demand cautious future analysis.

224 Many factors account for osteopathologies such as congenital, developmental, metabolic, diet, age,
225 traumatic injuries (summarised in Galateanu et al., 2013). However, captivity in enclosures with limited
226 space for the animals to remain athletic, and exposure to hard concrete for long hours may exacerbate foot
227 disease even if not the primary cause. To better understand foot pressures in rhinoceroses and the links to
228 foot disease, more *in vivo* locomotor data are required; ideally from multiple species and management
229 regimes.

230 Contrary to elephants that can easily be trained to walk over a walkway lined with pressure plates using
231 food as encouragement, rhinoceroses are seldom well-trained, so *in vivo* data collection is challenging. We
232 initially collected data on five animals but only a limited number of trials from this study's three individuals
233 could be used for final analyses due to spatial (i.e. partial foot contacts) and temporal (i.e. starting data
234 collection after initial foot contact and/or terminating data collection before final foot contact) completeness
235 issues. We conducted a power analysis for a one-way ANOVA on our rhinoceros peak pressure data for
236 each foot, where omega-squared was used for the effect size, significance was set at 0.01 and power was
237 set at 0.8. The minimum number of rhinoceroses to achieve this power would be 8, 39, 29 and 13 for the
238 left forefoot, right forefoot, left hindfoot and right hindfoot datasets respectively. Considering accessibility
239 and experimental limitations, it will be difficult (if not impossible) to recruit enough rhinoceroses (>40
240 considering that some subjects would need to be discarded from any study) from the same captive setting
241 for a statistically robust experiment.

242 Habitat loss and poaching have brought many rhinoceros species, in particular the Javan and the Sumatran,
243 to the brink of extinction (Crosta et al., 2017). Despite on-going legal and conservation efforts to protect
244 rhinoceroses, the number of populations impacted by poaching has increased dramatically over the last
245 two decades, with South Africa being affected the most due to having the largest number of rhinoceroses
246 in the world (Charlton 2017; Crosta et al., 2017). One of the measures in place to protect these animals
247 from extinction is to keep and breed them in captivity. While in captivity, they may develop foot disorders,
248 in particular chronic foot diseases, osteoarthritis, bone remodelling, osteitis-osteomyelitis, pododermatitis,
249 abscesses, and fractures (Galateanu et al., 2013; Jacobsen 2002; Regnault et al., 2013; von Houwald &
250 Flach 1998) that compromise animal welfare or even cause mortality due to being painful, progressive
251 and often untreatable. Even in wild rhinoceroses, there are reports of serious foot disease (Zainuddin et
252 al., 1990), and a high incidence of osteopathology appears to be an ancestral evolutionary trait for the
253 lineage, which may complicate efforts to improve the welfare of rhinoceroses (Stilson et al., 2016). To
254 date, most focus on appendicular pathologies in extant rhinoceroses have been on the feet, but the latter
255 study's finding that pathologies have been equally prevalent across the limbs throughout the ~50 million
256 year history of Rhinocerotidae raises questions of whether more proximal limb pathologies remain
257 common but overlooked in captive rhinoceroses. Follow-up studies should investigate this question and

258 even integrate it with biomechanical analyses to test whether some regional mechanical stresses are
259 unusually high in proximal elements and corresponding with locations predisposed to pathologies. Pond
260 and Alexander (1992) used a very simple analysis to estimate that femur stresses and safety factors were
261 high in galloping White rhinoceroses but this method certainly is imprecise, and stresses in humerus or
262 zeugopodial elements are unknown--- as are any joint contact stresses, which should be more important
263 for pathologies.

264

265 Disease management in large mammals such as elephants and rhinoceroses can be challenging and
266 examination using diagnostic approaches requires general anaesthesia or sedation, which can have negative
267 effects on the animal (Gage 2006; Hittmair & Vielgrader 2000; Siegal-Willott et al., 2012; von Houward &
268 Flach 1998). These challenges, coupled with the fact that foot diseases may only clearly manifest themselves
269 when they have progressed to advanced stages, can make euthanasia an unavoidable outcome (e.g. Jones
270 1979; Mikota 1999; Mikota et al., 1994). The causes of foot pathologies are multifactorial (e.g. Csuti et al.,
271 2001), but the biomechanical pressures imposed during locomotion presumably can promote or worsen
272 them. How can we thus protect rhinoceroses from developing foot diseases, or monitor treatment vs.
273 progression of chronic foot disease? An important step is to learn how rhinoceros feet function in captivity.
274 A valuable follow-on step would be to examine how husbandry conditions in captivity affect innate foot
275 function. Nevertheless, whilst we have a fair understanding of elephant foot pressures from captive and
276 semi-wild settings (Panagiotopoulou et al., 2012; 2016), here we have added new data on the pressures that
277 White rhinoceroses routinely apply to their feet during normal locomotion, and these give tentative insights
278 into not only basic biomechanics but also potential links of normal form and function vs. mechanically-
279 induced foot disease.

280
281

288

289 **Figure 1.** A. Image of Subject 3 walking on the pressure plate in the experimental walkway. B. Schematic
290 representation of the anatomical location of the nine regions of interest (ROI) across the left and right
291 fore- and hindfeet.

292 **Figure 2**. Scatter plot of peak foot pressure data from all three subjects at the nine regions of interest
293 (ROI) across the left forefoot, right forefoot, left hindfoot and right hindfoot respectively. Black line
294 represents the median pressure found at each ROI.

295 **Table 1**. Subject characteristics (*Ceratotherium simum*).
296
297 **Figure 3**. Peak pressure patterns during the whole stance phase of the left forefoot of all subjects.
298
299 **Figure 4**. Peak pressure patterns during the whole stance phase of the right forefoot of all subjects.
300
301 **Figure 5**. Peak pressure patterns during the whole stance phase of the left hindfoot of all subjects.
302
303 **Figure 6**. Peak pressure patterns during the whole stance phase of the right hindfoot of all subjects.

304

305 **Supplementary Data 1:** Regional peak pressure data for all subjects and feet. Columns A-J show

306 respectively the file name (A), subject ID (B), foot ID (C: left forefoot = 1; right forefoot = 2; left

307 hindfoot = 3; right hindfoot = 4); ROI (D; also see Figure 1); peak pressure data in N cm^{-2} (E); walking

308 speed in m s^{-1} (F); Shoulder height in metres (G); Froude number (H); Age (I; Adult=1; juvenile=2);

309 Body mass estimate in kg (J; 1 = 2500; 2 = 1000). Some trials were excluded from further analyses due to

310 being temporally incomplete. These are: [FORE LEFT: subject 1, trial 028_img001], [FORE RIGHT:

311 subject 3, trial 033_img004; subject 3, trial 035_img003], HIND LEFT: subject 3, trial 010_img003],

312 [HIND RIGHT: subject 3, trial 041_img006; subject 1, trial 001_img002; subject 1, trial 013_img005].

313 **Supplementary Figure S1**: Image time series of the COP trajectories (light grey) for the left forefoot of

314 subject 1 (010_img002 [A] and 027_img002 [B]).

315 **Supplementary Figure S2**: Image time series of the COP trajectories (light grey) for the left forefoot of

316 subject 2 (trials 018_img005 [A], 021_img005 [B] and 031_img002 [C]).

317 **Supplementary Figure S3**: Image time series of the COP trajectories (light grey) for the right forefoot of

318 subject 1 (trials 27_10_035_img002 [A] and 27_10_img002 [B]).

319 **Supplementary Figure S4**: Image time series of the COP trajectories (light grey) for the right forefoot of

320 subject 2 (trials 004_img007 [A], 009_img006 [B], 011_img004 [C] and 033_img003 [D]).

321 **Supplementary Figure S5**: Image time series of the COP trajectories (light grey) for the left hindfoot of

322 subject 1 (trials 27_10_038_img005 [A] and 014_img002 [B]).

323 **Supplementary Figure S6:** Image time series of the COP trajectories (light grey) for the left hindfoot of

324 subject 2 (trial 026_img004).

325 **Supplementary Figure S7**: Image time series of the COP trajectories (light grey) for the left hindfoot of

326 subject 3 (trial 034_img003).

327 **Supplementary Figure S8**: Image time series of the COP trajectories (light grey) for the right hindfoot of

328 subject 1 (trials 27_10_037_img003 [A] and 032_img003 [B]) and subject 2 (trial 27_10_019_img001 [C]).

329

330

331 **References**

332 Alexander RM, Pond CM. 1992. Locomotion and bone strength of the white rhinoceros, *Ceratotherium*

333 *simum*. Journal of Zoology 227(1): 63-69

334

335 Alexander RMN, Jayes AS. 1983. A dynamic similarity hypothesis for the gaits of quadrupedal

336 mammals. Journal of Zoology 201: 135–152 (doi:10.1111/j.1469-7998.1983.tb04266.x)

337

338 Charlton RW. 2017. Death and destruction: insight into the rhino poaching epidemic in South Africa.

339 Illinois State University. *Theses and Dissertations*. 661. https://ir.library.illinoisstate.edu/etd/661

340

341 Chi KJ, Roth VL. 2010. Scaling and mechanics of carnivoran footpads reveal the principles of footpad
342 design. Journal of the Royal Society Interface 7(49): 1145-1155

343

344 Crosta A, Sutherland K, Talerico C. 2017. Grinding rhino: An undercover investigation on rhino horn

345 trafficking in China and Vietnam. Elephant Action League Report

346

347 Csuti B, Sargent EL, Bechert US. 2001. *The elephant's foot: prevention and care of foot conditions in*

348 *captive Asian and African elephants*. Ames, IA: Iowa State University Press.

349

350 Dudley RJ, Wood SP, Hutchinson JR, Weller R. 2014. Radiographic protocol and normal anatomy of the

351 hind feet in the white rhinoceros (*Ceratotherium simum*). Veterinary Radiology & Ultrasound 56 (2):

352 124-132 (doi.org/10.1111/vru.12215)

353

354 Flach E, Walsh T, Dodds J, White A, Crowe O. 2003. Treatment of osteomyelitis in a greater one-horned

355 rhinoceros (*Rhinoceros unicornis*). Verh.Erkrg. Zootiere 41: 1–7

356

357 Fowler ME, Mikota SK. 2006. *Biology, medicine, and surgery of elephants*. Ames, IA: Blackwell

358 Publishing Ltd.

359

360 Gage L. 2006. *Radiology*. In: Fowler ME, Mikota SK, editors. Biology, Medicine, and Surgery of

361 Elephants. Ames, IA: Blackwell Publishing. pp. 192–197

362

363 Galateanu G, Hildebrandt TB, Maillot A, Etienne P, Potier R, Mulot B, Saragusty J, Hermes R. 2013.

364 One small step for rhinos, one giant leap for wildlife management- imaging diagnosis of bone pathology

365 in distal limb. Plos One 8(7): e68493 (doi: 10.1371/journal.pone.0068493)

366

367 Groves CP. 1972. *Ceratotherium simum*. Mammalian species 8: 1-6.

368

369 Harrison T, Stanley B, Sikarskie J, Bohart G, Ames N, Tomlian J, Marquardt M, Marcum A, Kiupel M,

370 Sledge D, Agnew D. 2011. Surgical amputation of a digit and vacuum-assisted-closure (V.A.C.)

371 management in a case of osteomyelitis and wound care in an eastern black rhinoceros (*Diceros bicornis*

372 *michaeli*). Journal of Zoo and Wildlife Medicine 42: 317–321

373

374   Hillman-Smith, AKK, Owen-Smith N, Anderson JL, Hall-Martin AJ, Selaladi JP. 1986. Age estimation of

375   the white rhinoceros (*Ceratotherium simum*). Journal of Zoology 210 (3): 355-377 (doi: 10.1111/j.1469-

376   7998.1986.tb03639.x)

377

378   Hittmair KM, Vielgrader HD. 2000. Radiographic diagnosis of lameness in African elephants (*Loxodonta*

379   *africana*). Veterinary Radiology & Ultrasound 41 (6):511-515

380

381   Hutchinson JR, Delmer C, Miller CE, Hildebrandt T, Pitsillides AA, Boyde AJ. 2011. From flat foot to fat

382   foot: the structure, ontogeny, function and evolution of elephant 'sixth toes'. Science 344: 1699–1703

383   (doi:10.1126/science.1211437)

384

385   Jacobsen J. 2002. *A Review of Rhino Foot Problems*. In: Proc. 2nd Rhino Keepers' Workshop 2001.

386   Zoological Society of San Diego, San Diego, California. Pp. 56–59.

387

388   Jones D. 1979. The husbandry and veterinary care of captive rhinoceroses. International Zoo Yearbook

389   19: 239–250

390

391   Lord M, Reynolds DP, Hughes JR. 1986. Foot pressure measurement: a review of clinical findings. Journal

392   of Biomedical Engineering 8: 283-294.

393

394   Mariappa D. 1986. Anatomy and histology of the Indian elephant. Oak Park, MI: Indira Publishing House.

395

396   Michilsens F, Aerts P, Van Damme R, D'Août K. 2009. Scaling of plantar pressures in mammals. Journal

397   of Zoology 279(3): 236-242.

398

399   Mikota SK, Sargent EL, Ranglack GS. 1994. *Medical Management of the Elephant*. Indira Publishing

400   House, West Bloomfield, Michigan.

401

402   Mikota SK. 1999. *Diseases of the elephant: a review*. In Erkrankungen der Zootiere: Verhandlungsbericht

403   des 39. Internationalen Symposiums uber die Erkrankungen der Zoo undWildtiere, pp. 1–15.

404

405   Miller MA, Hogan JN, Meehan CL. 2016 Housing and demographic risk factors impacting foot and

406   musculoskeletal health in African elephants (*Loxodonta africana*) and Asian elephants (*Elephas maximus*)

407   in North American Zoo. PLoS ONE 11, e0155223. (doi:10.1371/journal.pone.0155223)

408

409   Neuville H. 1935. Sur quelques caractères anatomiques du pied des éléphants. Arch Mus Natl d'Histoire

410   Naturelle, Paris, 6 e Série 13: 111–183

411

412   Owen-Smith RN. 1992. *Megaherbivores: the influence of very large body size on ecology*. Cambridge

413   university press.

414

415   Panagiotopoulou O, Pataky TC, Day M, Hensman MC, Hensman S, Hutchinson JR, Clemente CJ. 2016.

416   Foot pressure distributions during walking in African elephants (*Loxodonta africana*). Royal Society Open

417   Science 3:160203 (http://dx.doi.org/10.1098/rsos.160203)

418

419   Panagiotopoulou O, Pataky TC, Hill Z, Hutchinson JR. 2012. Statistical parametric mapping of the regional

420   distribution and ontogenetic scaling of foot pressures during walking in Asian elephants (*Elephas

421   maximus*). Journal of Experimental Biology 215: 1584–1593 (doi:10.1242/jeb.065862)

422

423   Prothero DR. 2005. *Evolution of North American Rhinoceroses*. Cambridge University Press

424

425   Regnault S, Dixon JJI, Warren-Smith C, Hutchinson JR, Weller R. 2017. Skeletal pathology and variable

426   anatomy in elephant feet assessed using computed tomography. PeerJ 5:e2877 (doi:10.7717/peerj.2877)

427

428   Regnault S, Hermes R, Hildebrandt T, Hutchinson J, Weller R. 2013. Osteopathology in the feet of

429   rhinoceroses: lesion type and distribution. Journal of Zoo and Wildlife Medicine 44: 918–927 (doi:

430   10.1638/2012-0277R1.1 PMID: 24450050)

431

432   Siegal-Willott JL, Alexander A, Isaza R. 2012. *Digital Radiography of the Elephant Foot*. In: Fowler ME,

433   Miller RE, editors. Zoo and Wild Animal Medicine, Current Therapy. St. Louis, Missouri: Elsevier

434   Saunders. pp. 515–523

435

436   Stilson KT, Hopkins SSB, Davis EB. 2016. Osteopathology in Rhinocerotidae from 50 Million Years to

437   the Present. PLoS ONE 11(2): e0146221 (doi:10.1371/journal.pone.0146221)

438

439   von Houwald F, Flach EJ. 1998. Prevalence of chronic foot disease in captive greater one-horned

440   rhinoceros (*Rhinoceros unicornis*). EAZWV Sci. Meet 2: 323-327.

441

442   von Houwald F, Guldenschuh G. 2002. *Husbandry manual for the greater one-horned or Indian*

443   *rhinoceros (Rhinoceros unicornis)* Linne, 1758. Basel Zoo, Basel, Switzerland.

444

445   von Houwald F. 2001. Foot problems in Indian rhinoceroses (*Rhinoceros unicornis*) in zoological gardens:

446   macroscopic and microscopic anatomy, pathology,and evaluation of the causes. Ph.D. dissertation, Univ.

447   of Zurich, Zurich, Switzerland

448

449   Weissengruber GE, Egger GF, Hutchinson JR, Groenewald HB, Elsasser L, Famini D, Forstenpointner G.

450   2006. The structure of the cushions in the feet of African elephants (*Loxodonta africana*). Journal of

451   Anatomy 209: 781–792 (doi:10.1111/j. 1469-7580.2006.00648.x)

452

453   Zainuddin ZZ, Abdullah MT, Shamsuddin M, Suri M. 1990. The husbandry and veterinary care of

454   captive Sumatran rhinoceros at Zoo Melaka, Malaysia. Malayan Nature Journal (Malaysia).

455
456
457
458
459
460
461
462

Figure 1

A. Image of Subject 3 walking on the pressure plate in the experimental walkway. B. Schematic representation of the anatomical location of the nine regions of interest (ROI) across the left and right fore- and hindfeet
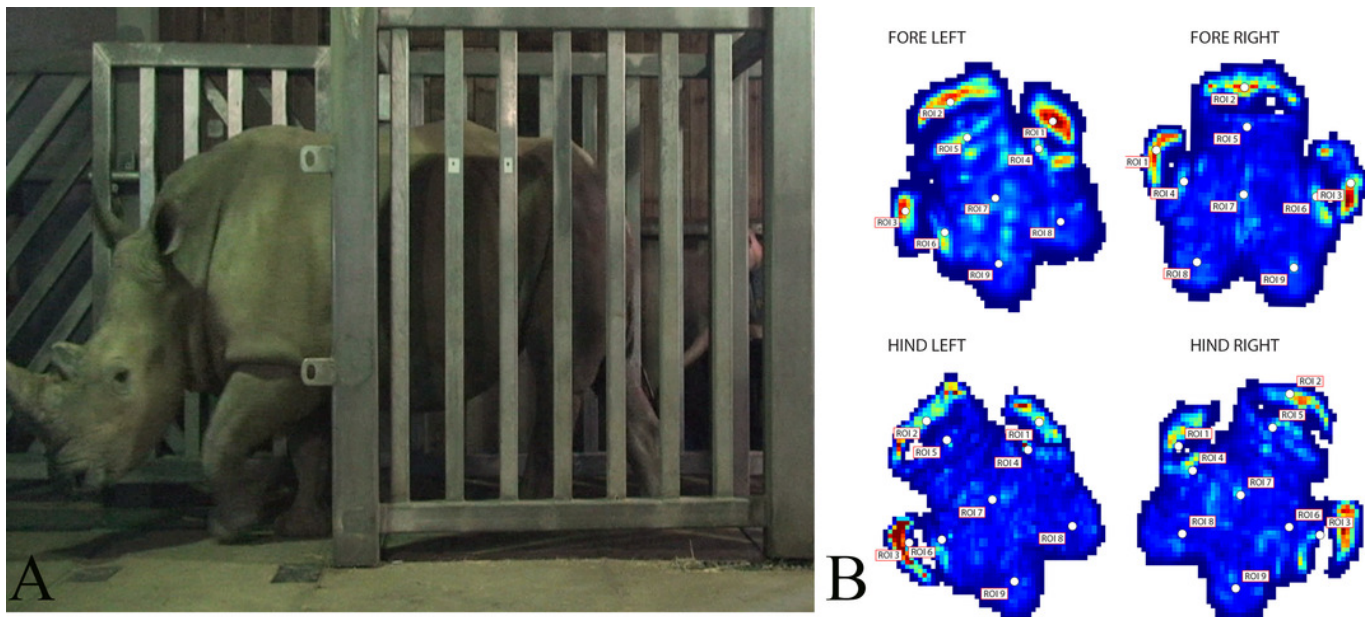
Figure 2(on next page)

Scatter plot of peak foot pressure data from all three subjects at the nine regions of interest (ROI) across the left forefoot, right forefoot, left hindfoot and right hindfoot respectively.
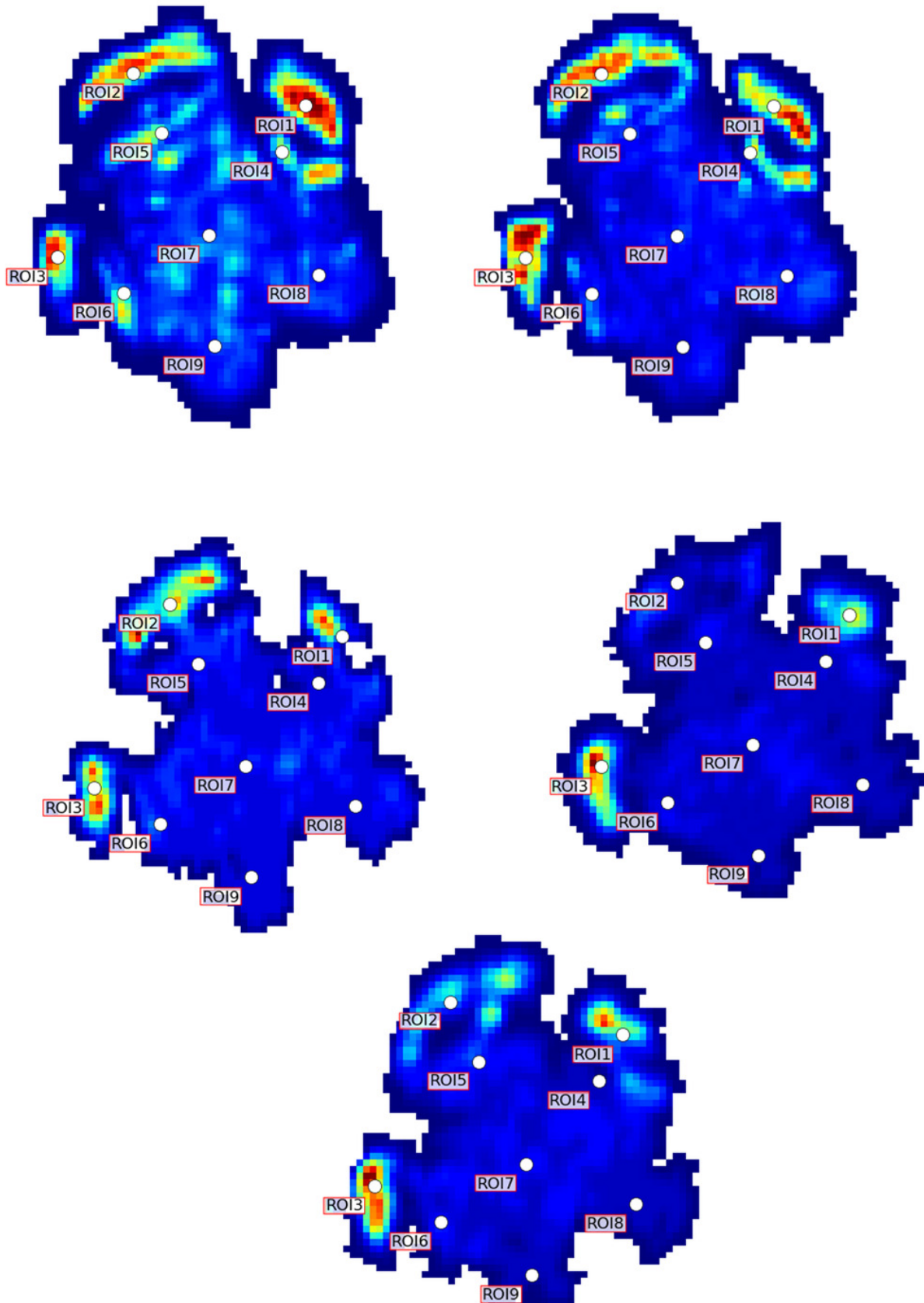
Black line represents the median pressure found at each ROI.
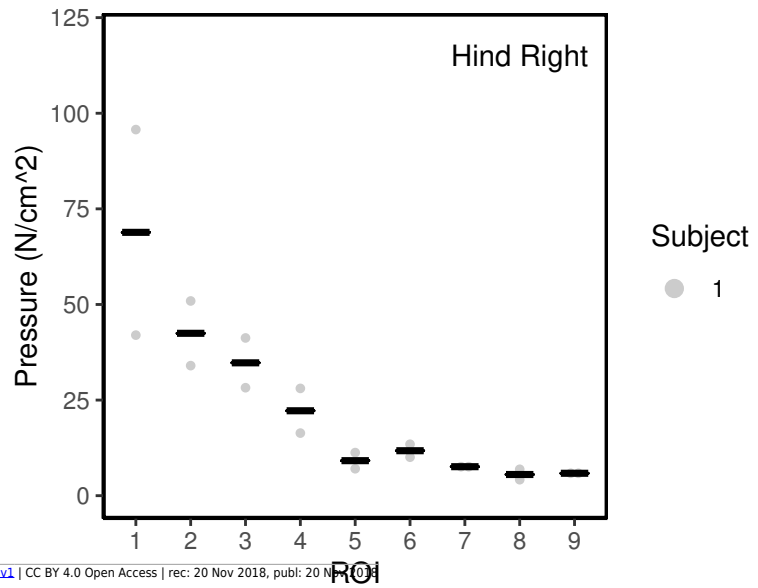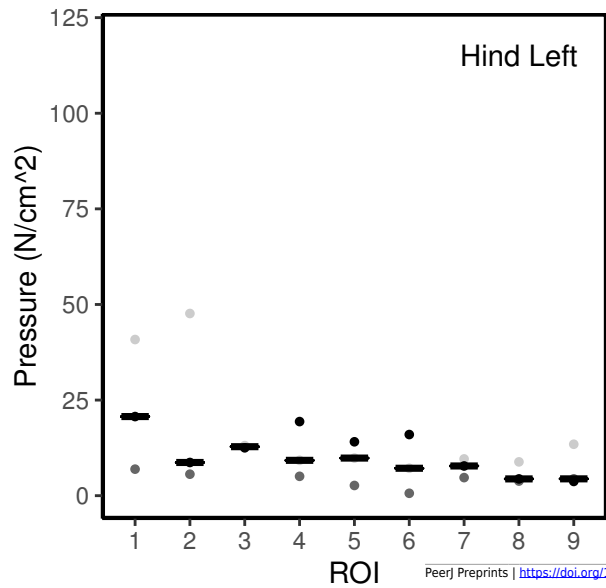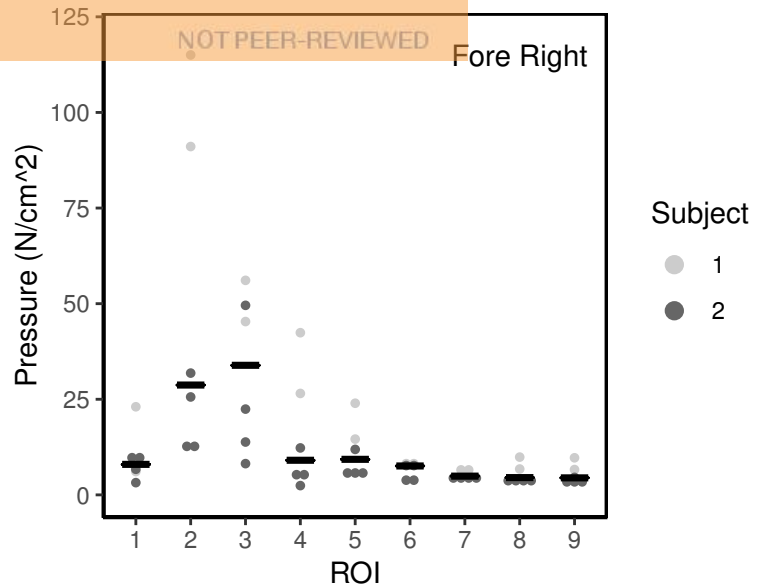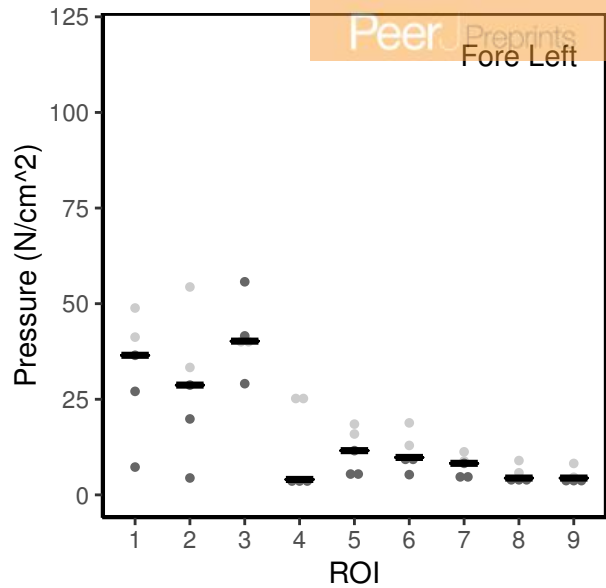
Figure 3

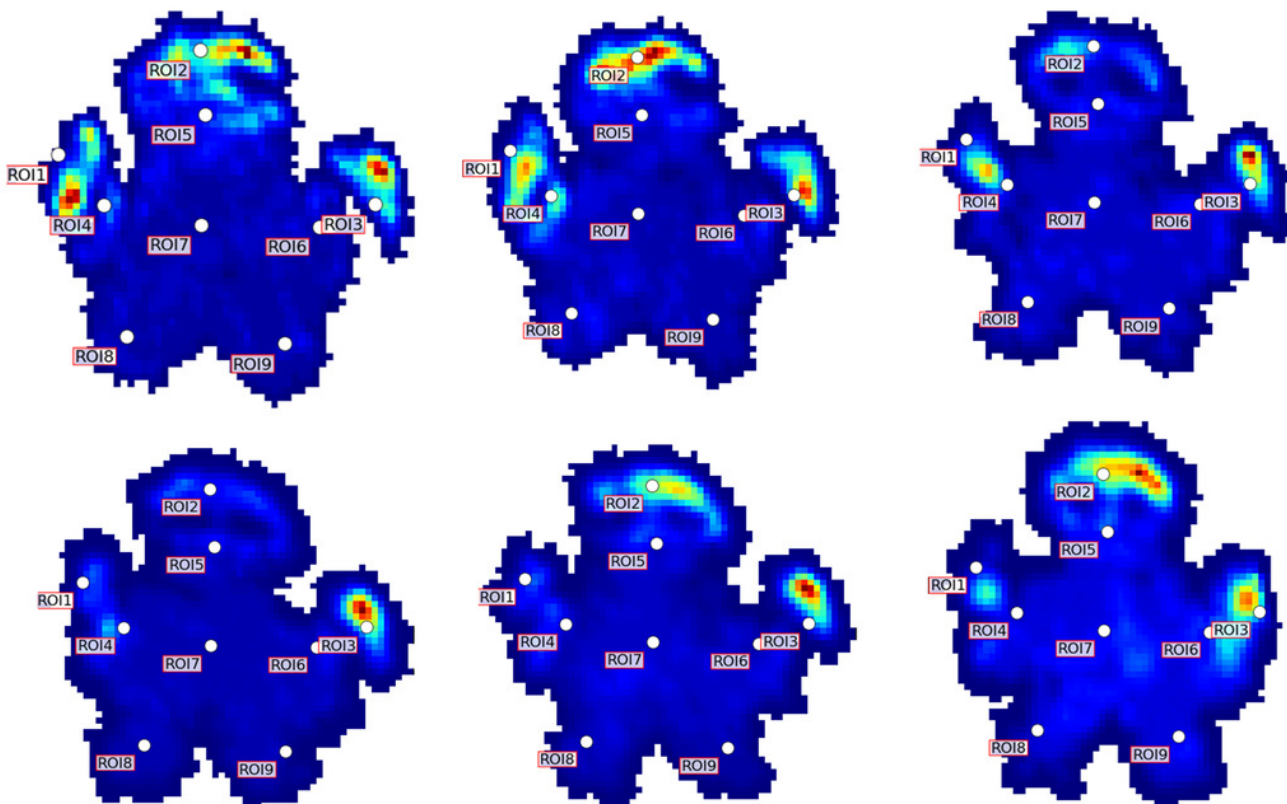Peak pressure patterns during the whole stance phase of the left forefoot of all subjects.
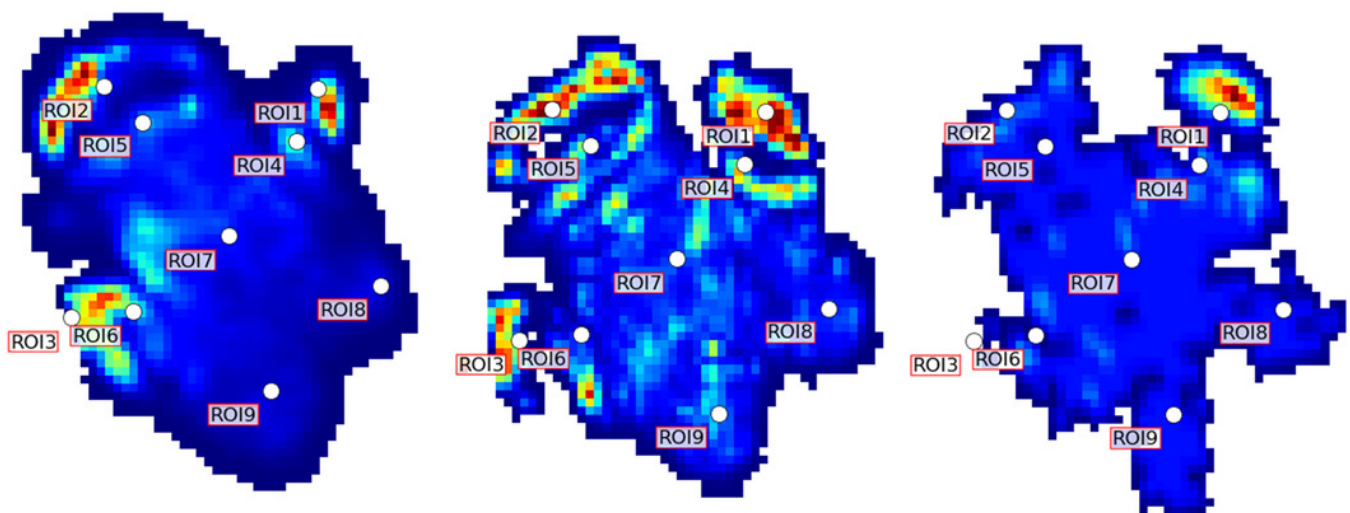
Fore Left

Figure 5

Peak pressure patterns during the whole stance phase of the left hindfoot of all subjects.

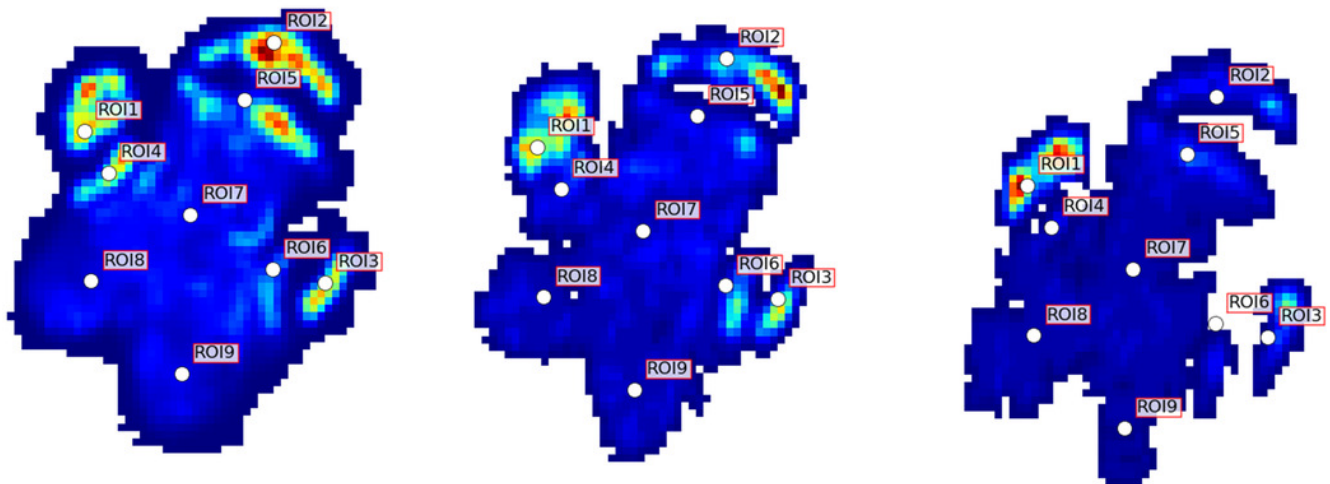Peer Preprints

Figure 6

Peak pressure patterns during the whole stance phase of the right hindfoot of all subjects.

Hind Right

Peer Preprints

Table 1(on next page)

Subject characteristics (*Ceratotherium simum*).

1   Table 1. Subject characteristics (*Ceratotherium simum*).
2

	Subject 1	Subject 2	Subject 3
Age	Adult	Juvenile	Adult
Sex	Female	Female	Female
Body mass (kg)- estimated	2500	1000	2500
Shoulder height (m)	1.5	0.65	1.42
Mean Froude number	0.014	0.001	0.054
Mean velocity (ms^{-1})	0.46	0.60	0.87
Mean maximum pressure (N cm^{-2}) Fore Left 1	23	13	No spatially/temporally complete data
Mean maximum pressure (N cm^{-2}) Fore Right 2	28	9	No spatially/temporally complete data
Mean maximum pressure (N cm^{-2}) Hind Left 3	18	4	12
Mean maximum pressure (N cm^{-2}) Hind Right 4	2	No spatially/temporally complete data	No spatially/temporally complete data
Number of Steps	4	3	1

3
4
5
6
7
8
9
10
11
12
13
14
15
16
17
18
19
20
21
22
23
24

25
26
27
28
29
30
31
32
33
34
35
36
37
38